

Original Article

Intestinal Metrnl released into the gut lumen acts as a local regulator for gut antimicrobial peptides

Zhi-yong LI[#], Mao-bing FAN[#], Sai-long ZHANG, Yi QU, Si-li ZHENG, Jie SONG, Chao-yu MIAO^{*}

Department of Pharmacology, Second Military Medical University, Shanghai 200433, China

Aim: Metrnl is a novel secreted protein, but its physiological roles remain elusive. In this study, we investigated the tissue expression pattern of Metrnl in humans and explored its possible physiological role in the tissues with most highly expressed levels.

Methods: A human tissue microarray containing 19 types of tissues from 69 donors was used to examine the tissue expression pattern of Metrnl, and the expression pattern was further verified in fresh human and mouse tissues. Intestinal epithelial cell-specific Metrnl knockout mice were generated, which were used to analyze the physiological roles of Metrnl.

Results: Metrnl was the most highly expressed in the human gastrointestinal tract, and was specifically expressed in the intestinal epithelium. Consistent with this, Metrnl mRNA was also most highly expressed in the mouse gastrointestinal tract among the 14 types of tissues tested. In the intestinal epithelial cell-specific Metrnl knockout mice, the Metrnl levels in the gut fluid were significantly reduced, whereas the Metrnl serum levels showed a trend towards a reduction, but this change was not statistically significant. This cell-specific deletion of Metrnl did not affect body weight, food intake, blood glucose, colon length and histology, intestinal permeability, mucus content or mucin 2 expression under physiological conditions, but statistically decreased the expression of antimicrobial peptides, such as regenerating islet-derived 3 gamma (Reg3g) and lactotransferrin.

Conclusion: Metrnl is highly expressed in the intestinal epithelial cells of humans and mice, which mainly contributes to the local gut Metrnl levels and affects the serum Metrnl level to a lesser extent. Metrnl plays a role in maintaining gut antimicrobial peptides.

Keywords: Metrnl; secreted protein; human expression pattern; intestine; epithelial cells; gut antimicrobial peptide

Acta Pharmacologica Sinica (2016) 37: 1458–1466; doi: 10.1038/aps.2016.70; published online 15 Aug 2016

Introduction

Metrnl, also known as Cometin^[1], Subfatin^[2], or Interleukin 39^[3], was recently identified as a secreted protein containing 311 amino acids with a 45-amino-acid signal peptide. Until now, there have only been a few studies exploring the function of Metrnl^[1, 4–6].

Metrnl has a similar function to its only homologous gene, Meteorin (Metrn), which is a novel neurotrophic factor^[7]. It has been demonstrated that recombinant Metrnl protein can accelerate neurite outgrowth and neuroblast migration *in vitro* and display a neuroprotective effect *in vivo*^[1].

We identified Metrnl as a novel adipokine during a process to screen new adipokines, demonstrating that Metrnl is abundant in subcutaneous adipose tissue in both humans and mice^[2]. Metrnl expression is dramatically increased during adipogenesis and in white fat during obesity. Through gener-

ation of adipose-specific Metrnl transgenic overexpression and knockout mice, we demonstrate that Metrnl can upregulate PPAR γ ; promote white adipocyte differentiation, expandability, and lipid metabolism; inhibit adipose inflammation; and ultimately antagonize obesity-induced insulin resistance^[6].

It has also been reported that Metrnl is upregulated in white adipose tissue upon acute cold exposure and in muscle after an acute bout of concurrent exercise. Administration of recombinant Metrnl protein or an adenovirus encoding the *Metrnl* gene promotes the transient browning of white adipose tissue through an eosinophil-dependent increase of IL-4 expression and alternative (M2) macrophage activation^[5], suggesting its role in immune-adipose interactions^[5]. A very recent study also implies that Metrnl is involved in both innate and acquired immune responses because Metrnl expression is upregulated in some human inflammation- or immune-associated diseases^[3].

Due to limited studies on Metrnl function, we are far from clear regarding the roles of Metrnl in various tissues. Furthermore, the tissue expression pattern of Metrnl in humans has not been examined at the protein level, although the tissue

[#]These authors contributed equally to this work.

^{*}To whom correspondence should be addressed.

E-mail cymiao@smmu.edu.cn

Received 2016-03-16 Accepted 2016-06-12

expression of *Metrn1* has previously been detected at the RNA level in our and other studies^[2, 3]. In this study, we examined the tissue expression pattern of *Metrn1* using human tissue microarray and found that *Metrn1* is very highly expressed in epithelial cells of the gastrointestinal tract, especially in the colon epithelium. Furthermore, we generated intestinal epithelial cell-specific *Metrn1* knockout mice to investigate the basic phenotypes of *Metrn1* in intestinal epithelial cells.

Materials and methods

Human multi-organ tissue microarray

A commercial tissue microarray (OD-NH-Com01-003) was purchased from Shanghai Outdo Biotech Co, Ltd and was constructed from formalin-fixed, paraffin-embedded human samples. The tissue microarray was prepared by dot-arraying 19 different types of tissues originating from 69 donors. The details of the samples are listed in Table 1.

Table 1. Information of the tissue microarray including 19 types of tissues from 69 donors.

Tissue type	Number of donors	Sex	Average age	Pathological diagnosis
Adrenal	4	M	35	Adrenal tissue
Brain	2	M	25	Cerebral cortex, hippocampus
Cerebellum	2	M	25	Cerebellar tissue
Large intestine	4	M/F	59	Rectum, colon
Small intestine	4	M/F	47	Small intestinal mucosa with chronic inflammation
Stomach	4	M	68	Gastric tissue
Kidney	4	M/F	42	Kidney tissue
Liver	4	M/F	49	Liver with chronic inflammation
Lung	4	M/F	40	Pulmonary tissue
Pancreas	4	M/F	43	Pancreatic tissue
Ovary	4	F	52	Ovarian tissue
Testis	4	M	35	Testis tissue
Prostate	4	M	46	Prostatic tissue with nodular hyperplasia
Uterus	4	F	47	Uterine tissue
Thyroid	4	M	35	Thyroid tissue with hyperplasia or chronic inflammation
Skeletal muscle	4	M	35	Striated muscle
Skin	4	M	35	Skin tissue
Heart	2	M	25	Left ventricular wall
Spleen	3	M/F	50	Spleen, spleen with chronic blood clot

All research involving human subjects was approved by the medical ethical committee of the Second Military Medical University, and written informed consent was obtained from all subjects.

Immunohistochemical staining for *Metrn1*

Immunohistochemical staining of human and mouse tissues using *Metrn1* antibody (Sigma) was performed on slides according to the protocol we previously described^[2, 6]. Briefly, slides were incubated at 60°C for 20 min. After routine deparaffinization and rehydration, the slides were pretreated with 10 mmol/L sodium citrate buffer (pH 6.0) and boiled for 10 min for antigen retrieval. The endogenous peroxidase was quenched by adding hydrogen peroxide (3% H₂O₂ in 100% ethanol) at room temperature for 15 min. After washing with phosphate buffered saline (PBS), the slides were blocked with 10% non-immune goat serum. Then, the slides were incubated overnight with primary *Metrn1* antibody (1:100 dilutions) and washed with Tris-buffered saline. Next, the slides were incubated with horseradish peroxidase-conjugated anti-rabbit IgG (1:1000) for 15 min. Immunoreactive complexes were detected with 3,3'-diaminobenzidine (DAB, Sigma). Finally, the slides were counter-stained with hematoxylin before microscopic analysis.

Generation of intestinal epithelial cell-specific *Metrn1* knockout mice

All animal experiments were performed in accordance with the National Institutes of Health Guide for the Care and Use of Laboratory Animals and were approved by the animal ethical committee of the Second Military Medical University. *Metrn1*^{loxP/loxP} mice were generated as we described elsewhere^[6]. Villin-cre mice [B6.Cg-Tg(Vil1-cre)1000Gum/J; JAX stock 021504] were used to generate intestinal epithelial cell-specific *Metrn1* knockout (*Metrn1*^{-/-}) mice. The breeding strategy for the *Metrn1*^{-/-} mice is displayed in Figure 2A. Briefly, *Metrn1*^{loxP/loxP} mice were crossed to Villin-cre mice to generate *Metrn1*^{loxP/wt} Villin-cre mice, which were crossed to *Metrn1*^{loxP/loxP} mice to generate *Metrn1*^{loxP/loxP} Villin-cre mice (*Metrn1*^{-/-} mice). Then, *Metrn1*^{-/-} mice were mated with *Metrn1*^{loxP/loxP} mice, and their offspring were genotyped by polymerase chain reaction (PCR) analysis of genomic DNA. The littermate *Metrn1*^{loxP/loxP} mice were used as the corresponding wild-type controls.

Detection of food intake and blood glucose

For the detection of food intake, the mice were placed in pairs in cages, and their food intake was monitored for 3 d. For the detection of blood glucose, mouse tail blood was used to measure the blood glucose levels at the basal state and at 2, 4, 6, 8, 10, and 12 h after fasting with OneTouch Glucose Meters (LifeScan), as described elsewhere^[8].

Fluorescein isothiocyanate-dextran assay

Wild-type and *Metrn1*^{-/-} mice were fasted for 4 h and then administered 10 mg of fluorescein isothiocyanate (FITC)-dextran (molecular weight, 3000–5000 Da or 40000 Da; Sigma) by gavage as described elsewhere^[9]. After 4 h, the mice were euthanized by cervical dislocation and bled by cardiac puncture. The blood was centrifuged at 3000×g for 30 min, and the

serum was collected for fluorometry at Ex/Em 485/528 nm to detect the fluorescence intensity.

Quantification of mRNA by real-time PCR

Total RNA was extracted from various tissues using TRIzol reagent (Invitrogen), and real-time PCR was performed using an ABI 7500 Real-Time PCR System (Applied Biosystems) as previously described^[2]. A final 20 μ L reaction mixture included 10 μ L SYBR Green, 2 μ L cDNA template and 1 μ L primers. The average threshold cycle (Ct) was determined from duplicate reactions, the target gene expression was normalized to GAPDH, and quantitative measurements were obtained using the $\Delta\Delta C_T$ method. All primers are listed with their sequences in Table 2.

Histological staining

Periodic acid-Schiff (PAS) and hematoxylin and eosin (H&E) staining were performed as previously described^[10,11]. Briefly, the intestine samples used for histological analysis were fixed with 4% phosphate buffered paraformaldehyde for 24 h and embedded in paraffin. Sections of 4- μ m thickness were prepared and stained with PAS or HE. Images were captured using a Leica microscope. Semiquantitative analysis of PAS staining was performed using ImageJ software.

Gut fluid collection

The method for intestinal fluid collection followed a previously described procedure^[12]. Briefly, after fasting overnight, mice were euthanized with an overdose of pentobarbital sodium^[13], and the abdomen was immediately opened to excise identical 5 cm lengths of colon. First, the colon samples were incubated with 8 mL PBS for 10 min. Second, a syringe with a blunt needle was used to flush PBS three times from the proximal to distal ends of the lumen of the colon. Then, the

PBS was collected and centrifuged at 12000 \times g at 4°C for 10 min. The supernatant was collected and filtered using Amicon® Ultra-4 Centrifugal Filters (molecular weight cutoff 10 kDa, Merck). The concentrated liquid was slightly adjusted to the same volume with PBS. Finally, the Metrnl concentration was determined using the DuoSet Development kit (R&D Systems).

Statistical analysis

All data are presented as the mean \pm SEM and were analyzed using Prism 5.0 software (GraphPad Software). Statistical significance was determined by a two-tailed Student's *t*-test. *P*<0.05 was considered to be statistically significant.

Results

High expression of Metrnl in the human gastrointestinal tract

To investigate the expression pattern of Metrnl in different human tissues, we performed multi-organ human tissue microarray. Most of the tissues evaluated comprised four samples from different donors with different ages. According to the results of immunohistochemical staining, the tissues could be divided into 4 grades: negative, weak positive, positive, and strong positive. As shown in Table 3, we did not detect Metrnl expression in the brain, cerebellum, skeletal muscle, ovary, prostate, heart, pancreas or uterus, which was in accordance with our previous study^[2]. The expression of Metrnl in the liver and adrenal glands was weakly positive. Metrnl was expressed in the kidney, thyroid, testis, spleen and lung. Notably, Metrnl expression in the gastrointestinal tract and skin was strongly positive and dramatically higher than that in other tissues (Table 3, Figure 1A).

To determine in which types of cells Metrnl expression occurred, more fresh human intestine tissues were collected, and Metrnl expression was detected with immunohistochem-

Table 2. Primer sets used in the study.

	Forward primer (5'-3')	Reversed primer (5'-3')
Genes for genotyping		
Floxed Metrnl (Metrnl ^{loxP/loxP})	TGAGGGTTGGAGGCTCTAGC	GGATGAGCGTTTGAGCACAGC
Cre (Villin-Cre)	GCGGTCTGGCAGTAAAACTATC	GTGAAACAGCATTGCTGCTCACTT
Genes for real-time PCR		
Metrnl	CTGGAGCAGGGAGGCTTATTT	GGACAACAAAGTCACTGGTACAG
GAPDH	GTATGACTCCACTCACGGCAAA	GGTCTCGCTCCTGGAAGATG
Villin1	TCAAAGGCTCTCTCAACATCAC	AGCAGTCACCATCGAAGAAGC
Mucin2	TGTGTTCACGGGAATGCTGAG	TGCAGGCGATGACGTTGAG
SAA3	TGCCATCATCTTTGCATCTTGA	CCGTGAACCTCTGAACAGCCT
Reg	ATGCTTCCCGTATAACCATCA	GGCCATATCTGCATCATACCAG
Reg3b	ACTCCCTGAAGAATATACCCTCC	CGCTATTGAGCACAGATACGAG
Lactotransferrin	TGAGGCCCTTGGACTCTGT	ACCCACTTTTCTCATCTCGTTC
Haptoglobin	GCTATGTGGAGCACTTGGTTC	CACCCATTGCTTCTCGTCTGTT
S100A8	AAATCACCATGCCCTCTACAAG	CCCCTTTTATCACCATCGCAA

SAA3, serum amyloid A-3; Reg3g, regenerating islet-derived 3gamma; Reg3b, regenerating islet-derived 3beta; S100A8, S100 calcium binding protein A8.

Table 3. Immunohistochemical staining for *Metrn1* in human tissue microarray.

Intensity of staining	Tissues
Strongly positive staining	Large intestine, small intestine, stomach, skin
Moderately positive staining	Kidney, thyroid, testis, spleen, lung
Weakly positive staining	Liver, adrenal
Nearly negative staining	Brain, cerebellum, skeletal muscle, ovary, prostate, heart, pancreas, uterus

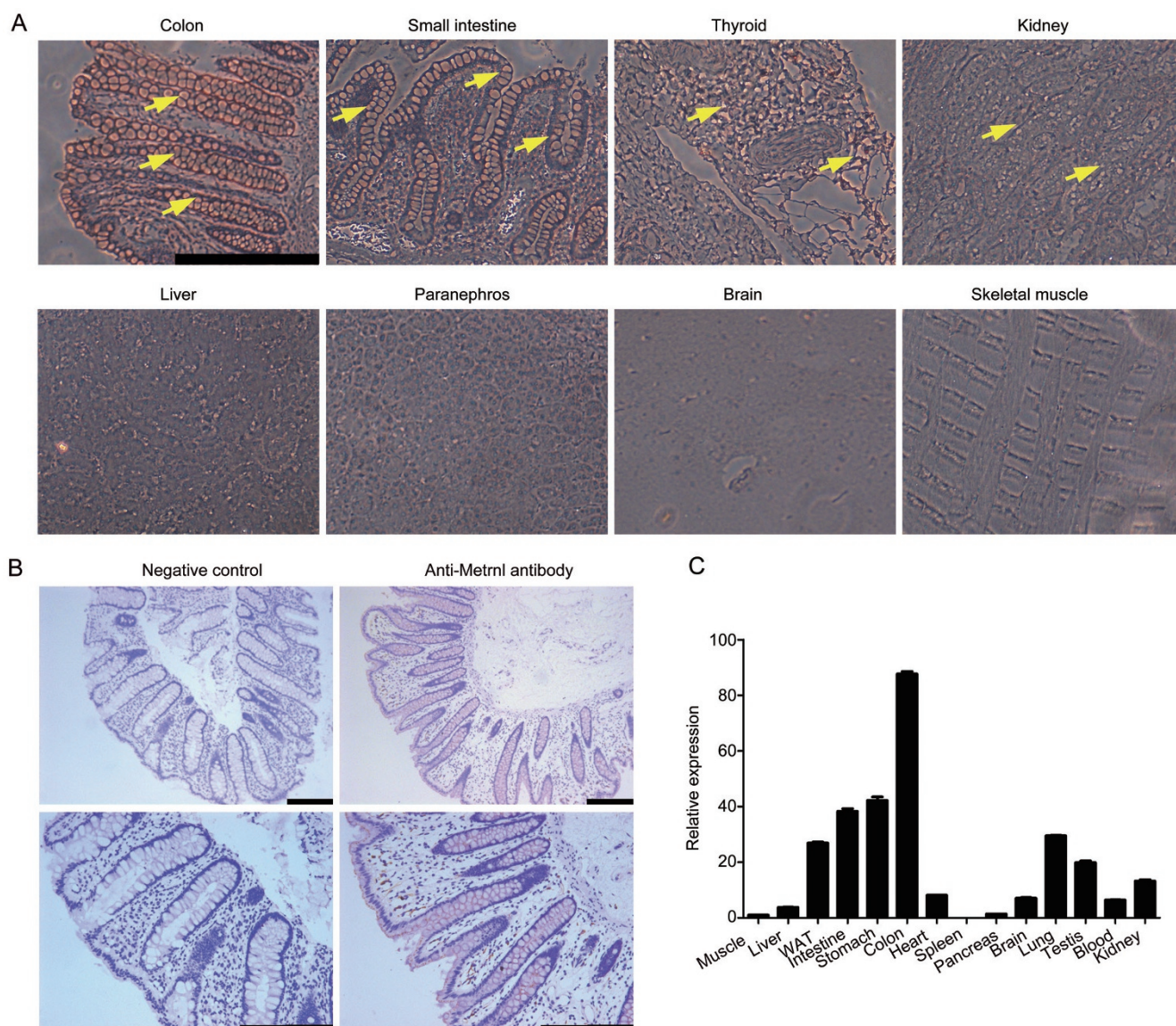


Figure 1. High expression of *Metrn1* in the gastrointestinal tracts of humans and mice. (A) Immunohistochemical staining of representative human tissues. Strong positive immunostaining in the colon and small intestine, moderate positive immunostaining in the thyroid and kidney, weak positive immunostaining in the liver and adrenal glands, and nearly negative immunostaining in the brain and skeletal muscle were observed. Bar, 50 μ m. Staining of *Metrn1* is indicated by a yellow arrow. (B) *Metrn1* expression in human intestinal epithelial cells. Bar, 200 μ m. (C) *Metrn1* mRNA expression in 14 tissues from C57BL/6 mice, with the highest expression in the colon, followed by the small intestine and stomach.

istry. The results showed that *Metrn1* was mainly expressed in the epithelial cells of the intestine but not in other cell types (Figure 1B).

To further identify whether *Metrn1* displays a similar expression pattern in the mouse, we detected *Metrn1* expression in different mouse tissues with real-time PCR. Consistently,

Metn1 expression was very high in the mouse gastrointestinal tract, especially in the colon. Metn1 expression in the adipose tissue, lung, testis and kidney was relatively high, whereas its expression in the brain, spleen or pancreas was much lower (Figure 1C).

Deficiency of Metn1 in intestinal epithelial cells does not cause visible differences

To understand the role of Metn1 in intestinal epithelial cells, we generated intestinal epithelial cell-specific Metn1 knockout mice by mating Metn1^{loxp/loxp} mice and Villin-cre mice (Figure 2A–2C). The knockout efficiency of Metn1 was evaluated by both real-time PCR and immunohistochemistry. Metn1 expression was reduced by 96% in the colon and showed no changes in the heart, liver, muscle and adipose tissue (Figure 2D). Consistent with this, immunohistochemical staining demonstrated that Metn1 protein expression in the colon epithelial cells of Metn1^{-/-} mice was much lower than that in wild-type mice (Figure 2E). These results confirmed that Metn1 in intestinal epithelial cells was specifically knocked out in Metn1^{-/-} mice.

The ratio of Metn1^{-/-} and Metn1^{loxp/loxp} mice followed Mendel's law, and no visible differences were observed between

the Metn1^{-/-} and wild-type mice. The body weight and food intake of Metn1^{-/-} mice showed no difference from wild-type mice (Figure 3A and 3B). The blood glucose levels were comparable between Metn1^{-/-} and wild-type mice under both fed and fasting conditions (Figure 3C).

We further measured the length of the large intestine, which was unchanged in Metn1^{-/-} mice (Figure 4A). We also did not observe histological differences between the intestines of Metn1^{-/-} and wild-type mice using H&E staining (Figure 4B). In addition, to test the influence of Metn1 on intestinal permeability, the fluorescence intensity of FITC in the serum was examined after gavage with FITC-conjugated dextran at different molecular weights. As shown in Figure 4C, no difference was found between Metn1^{-/-} and wild-type mice in either the small-molecular-weight dextran group or the high-molecular-weight dextran group.

Deficiency of Metn1 in intestinal epithelial cells reduces the Metn1 level in the gut fluid

Considering that the Metn1 protein existed in both the vesicles and cytoplasm of epithelial cells, it could be secreted into the blood and be exported into the gut fluid via exocytosis. To determine whether intestine epithelial cells are the major

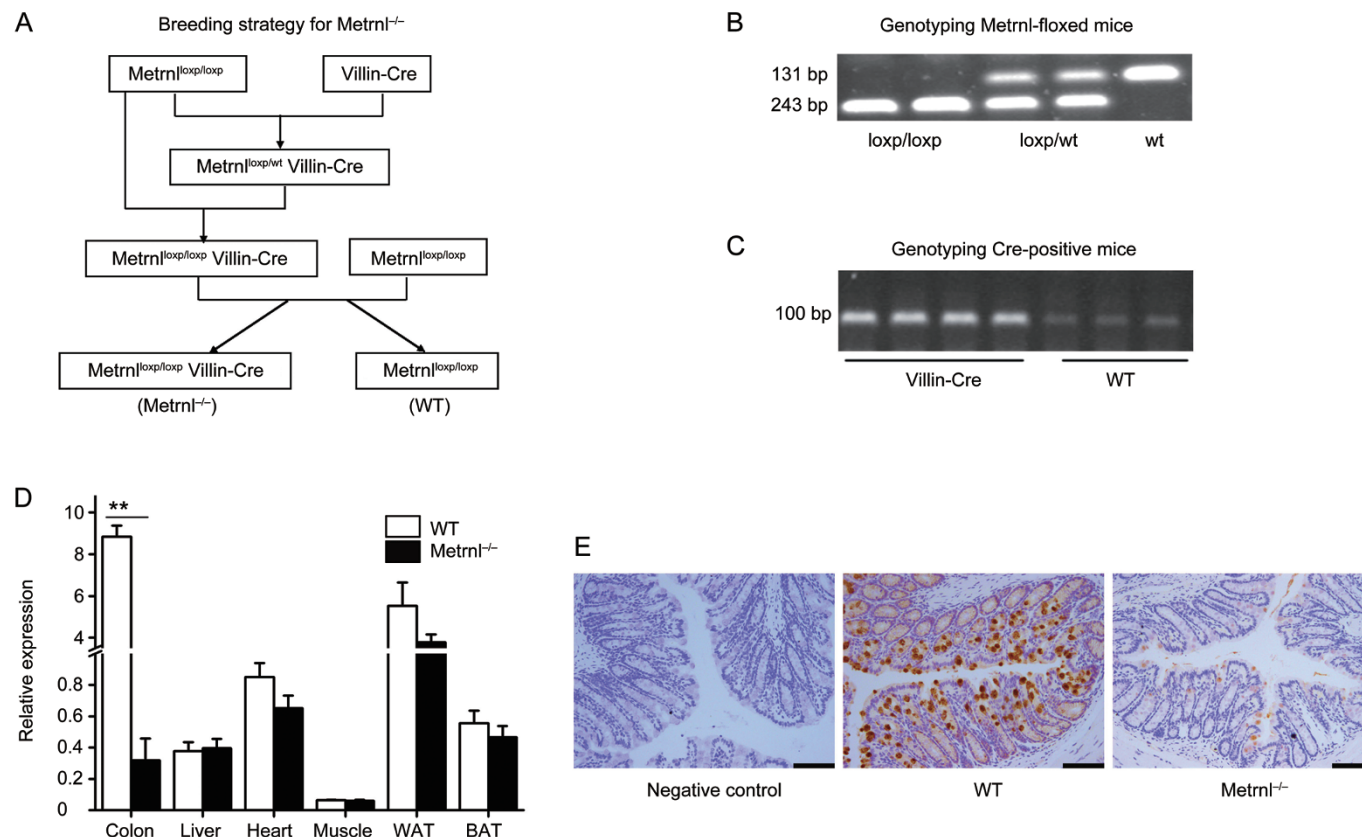


Figure 2. Breeding and identification of Metn1^{loxp/loxp} Villin-cre mice (Metn1^{-/-}). (A) Breeding strategy for Metn1 conditional knockout mice. (B) Genotyping of Metn1-floxed mice. The PCR product of 243 bp is amplified from the conditional floxed (loxp-flanked) Metn1 allele, and the PCR product of 131 bp is amplified from the wild-type Metn1 allele. (C) Genotyping of Cre-positive mice, including Metn1^{loxp/wt} Villin-cre and Metn1^{loxp/loxp} Villin-cre mice. (D) Metn1 mRNA expression in the tissues of Metn1^{-/-} and wild-type mice. WAT, white adipose tissue. BAT, brown adipose tissue. $n=6$. The data are expressed as the mean \pm SEM. ** $P<0.01$. (E) Immunohistochemical staining for Metn1 in the colons of Metn1^{-/-} and wild-type mice. Bar, 100 μ m.

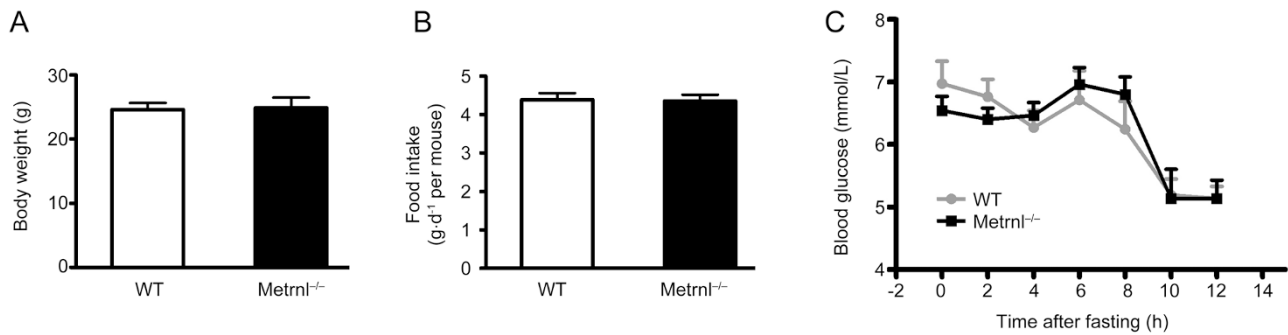


Figure 3. Effects of intestinal epithelial *Metnrl* on body weight, food intake and blood glucose. (A) The body weight of *Metnrl*^{-/-} mice is comparable to that of wild-type mice fed a normal chow diet. (B) Food intake of *Metnrl*^{-/-} and wild-type mice fed a normal chow diet. *n*=12. (C) Blood glucose levels were measured at the indicated time points after fasting in *Metnrl*^{-/-} and wild-type mice fed a normal chow diet. *n*=7. Mean±SEM.

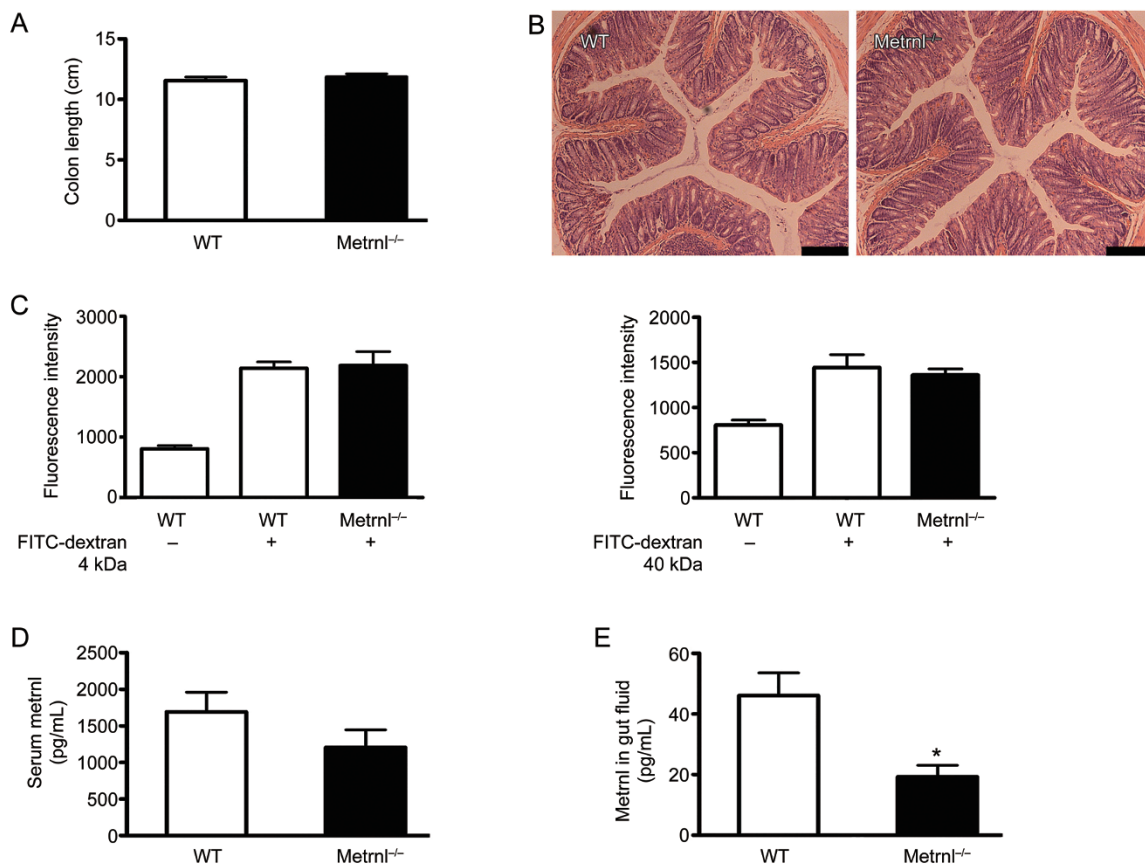


Figure 4. Effects of intestinal epithelial *Metnrl* on colon length, intestinal permeability and histology, serum *Metnrl* levels, and the level of *Metnrl* in the gut fluid. (A) *Metnrl*^{-/-} mice display no difference in colon length compared with wild-type mice. (B) H&E staining of the colon in *Metnrl*^{-/-} and wild-type mice. Bar, 200 μm. (C) The fluorescence intensity of FITC in the serum is comparable between *Metnrl*^{-/-} and wild-type mice after gavage with FITC-conjugated dextran at the indicated molecular weight. (D) The serum concentration of *Metnrl* tended towards a decrease in *Metnrl*^{-/-} mice compared to wild-type mice. *n*=7. (E) The *Metnrl* level in the gut fluid is significantly reduced in *Metnrl*^{-/-} mice. *n*=7. The data are expressed as the mean±SEM. **P*<0.05.

source of circulating *Metnrl*, we compared the serum concentration of *Metnrl* between *Metnrl*^{-/-} and wild-type mice using an ELISA kit. As shown in Figure 4D, the *Metnrl* serum level tended towards being reduced in *Metnrl*^{-/-} mice but the differ-

ence was not significant. However, the *Metnrl* concentration in the gut fluid was significantly reduced in *Metnrl*^{-/-} mice (Figure 4E).

Deficiency of *Metrn1* in intestinal epithelial cells does not change mucin production but downregulates antimicrobial peptides

One of the major functions of epithelial cells is the secretion of mucus^[14–17]. To clarify whether *Metrn1* in epithelial cells regulates mucin expression, periodic acid-Schiff staining was performed, which showed that the mucus content in epithelial cells was not changed in *Metrn1*^{-/-} mice (Figure 5A). Mucin 2 is particularly prominent in the gut and is secreted by epithelial cells^[18–21]. Hence, we further detected mucin 2 expression with real-time PCR, finding that its expression was also unchanged (Figure 5B).

Intestinal epithelial cells, especially Paneth cells, produce a large number of antimicrobial peptides to prevent microorganism translocation and modulate microbial populations at the mucosal surface^[22, 23]. Thus, we further evaluated the expression of antimicrobial peptides in the intestine. As shown in Figure 5B, contrary to the lack of change in Villin expression in *Metrn1*^{-/-} mice, the expression of most antimicrobial peptides, such as regenerating islet-derived 3 gamma (*Reg3g*)^[24–26] and lactotransferrin^[27], was significantly decreased. Others, such as serum amyloid A-3 (*SAA3*)^[28] and regenerating islet-derived 3 beta (*Reg3b*)^[25, 29], showed a trend towards a decrease. This suggests that *Metrn1* plays a role in regulating the expression of antimicrobial peptides.

Discussion

In the present study, we demonstrated the expression pattern of *Metrn1* in various tissues, especially in human tissues. We found that *Metrn1* was abundantly expressed in both human and mouse gastrointestinal tracts. Immunohistochemistry results further demonstrated that *Metrn1* was mainly expressed in intestinal epithelial cells. To explore its function

in intestinal epithelial cells, we generated intestinal epithelial cell-specific *Metrn1* knockout mice. No visible difference was observed between *Metrn1*^{-/-} and wild-type mice. The body weight, food intake, blood glucose, length of the intestine, intestinal permeability and mucus secretion remained unchanged in *Metrn1*^{-/-} mice. The *Metrn1* serum level showed a tendency towards a decrease, but no significant difference was observed between *Metrn1*^{-/-} mice and wild-type mice. However, we indeed detected a significant reduction of the *Metrn1* level in the gut fluid and a marked downregulation of antimicrobial peptides in the intestinal tissue of *Metrn1*^{-/-} mice. During the process of measuring the tissue expression pattern of *Metrn1*, we found that *Metrn1* was extremely highly expressed in both the human and the mouse gastrointestinal tract. Using an immunohistochemistry method, we further identified that *Metrn1* was exclusively expressed in the epithelial cells of the intestine. Consistent with our finding, a previous study reported that *Metrn1* was highly expressed in barrier tissues^[3]. In accordance with this, we also found that *Metrn1* expression was abundant in the lung and skin. Conclusively, this study, combined with the previous reports from our and other labs^[1–3, 6], demonstrates that *Metrn1* expression is the highest in the gastrointestinal tract and skin, relatively high in white adipose tissue and the lung, and much lower in the muscles, spleen, pancreas and brain.

Intestinal epithelial cells are uniquely located at the border of luminal commensal microbiota and the lamina propria of the intestine^[30, 31]. Secretory intestinal epithelial cells can secrete mucins and antimicrobial proteins to establish a physical and biochemical barrier between the bacterial and epithelial surfaces^[22, 30]. To explore the function of *Metrn1* in intestinal epithelial cells, we generated intestinal epithelial

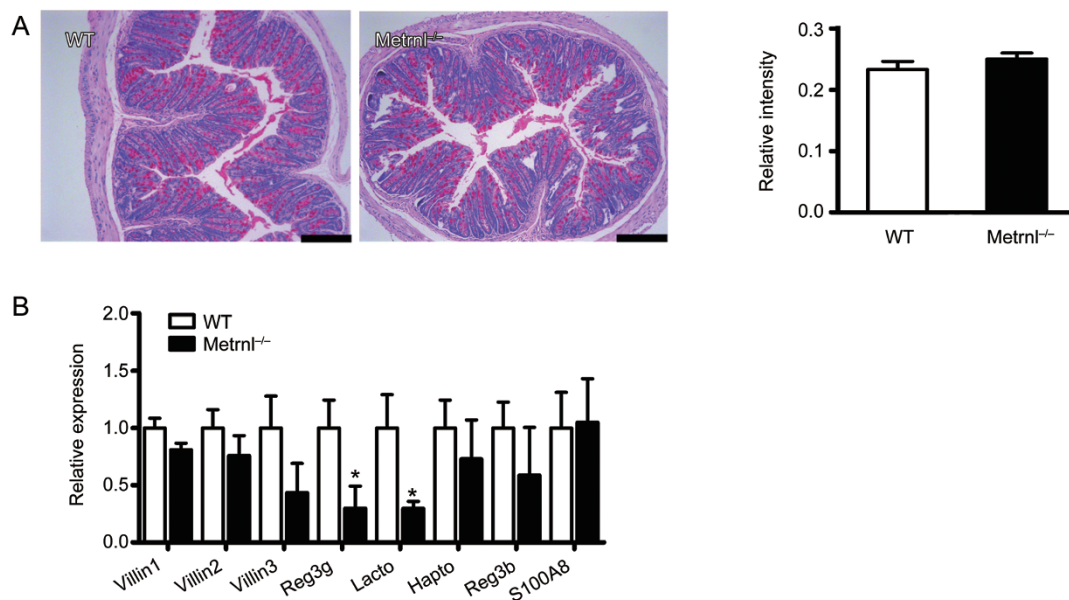


Figure 5. Effects of intestinal epithelial *Metrn1* on mucus production and antimicrobial gene expression. (A) Periodic acid-Schiff staining of the colon in *Metrn1*^{-/-} and wild-type mice. Semiquantitative analysis was performed using ImageJ software. $n=5$. Bar, 200 μm . (B) Relative expression of mucin 2 and antimicrobial genes in the colons of *Metrn1*^{-/-} and wild-type mice. $n=6$. The data are expressed as the mean \pm SEM. * $P<0.05$.

cell-specific *Metrn1* knockout mice. Body weight, food intake and blood glucose were not changed in these mice, suggesting that *Metrn1* may not significantly influence intestinal nutrient absorption under physiological conditions. The length, permeability and histology of the intestine were also not altered in *Metrn1* knockout mice, suggesting that *Metrn1* is unable to influence intestinal development and structure. Mucus content and mucin 2 expression in epithelial cells and the colon were also similar between *Metrn1* knockout and wild-type mice. Hence, *Metrn1* does not affect intestinal mucus secretion. However, our study observed that the ablation of *Metrn1* dramatically reduced the expression of several antimicrobial peptides, such as Reg3g and lactotransferrin, suggesting that *Metrn1* can regulate the production of antimicrobial peptides and may have a role in interactions between hosts and microorganisms. Because *Metrn1* is a secreted protein, it is unclear whether *Metrn1* changes antimicrobial peptide expression in a direct or indirect way. Thus, the specific mechanism still needs to be further explored.

Considering that *Metrn1* expression was the highest in the intestinal epithelium among the evaluated tissues, we wondered whether it is the major source of blood *Metrn1* in systemic circulation. The *Metrn1* serum level was not statistically and significantly decreased in *Metrn1*^{-/-} mice compared with wild-type mice, which does not support the notion that *Metrn1* released from intestinal epithelial cells is the main source of blood *Metrn1*. Correspondingly, the *Metrn1* level in the gut fluid was significantly decreased, indicating that *Metrn1* expressed in intestinal epithelial cells was mostly exported into the gut fluid. These results are consistent with the results of *Metrn1* immunohistochemistry in the intestine showing that *Metrn1* seems to exist mainly in exocytic vesicles (Figure 2E).

The function of *Metrn1* in intestinal epithelial cells or other mucous glands needs to be explored further. In this study, we showed that *Metrn1* regulated the expression of antimicrobial peptides. It has also been reported that *Metrn1* is upregulated in inflammatory disease and regulates immune cell aggregation and inflammatory factor release^[3, 5]. All these results, combined with the regulation of the local intestinal *Metrn1* level, suggest that *Metrn1* may participate in homeostasis of mucosal immunity and the development of inflammatory bowel disease, which need to be explored further.

In conclusion, we show that *Metrn1* is highly expressed in the intestinal epithelial cells of humans and mice. *Metrn1* can be secreted from intestinal epithelial cells, which mainly contributes to the local level of *Metrn1* in the gut, and has less of an effect on the systemic circulating level of *Metrn1*. *Metrn1* seems not to play a critical role in intestinal development, nutrient absorption, or mucus secretion. However, *Metrn1* can significantly regulate the intestinal production of antimicrobial proteins.

Acknowledgements

This study was supported by grants from the National Natural Science Foundation of China (No 81130061, 81202572, and 81373414) and Shanghai Science and Technology Innovation

Action Plan (No 16JC1405100).

Author contribution

Chao-yu MIAO designed the study and revised the manuscript; Zhi-yong LI and Mao-bing FAN wrote the manuscript; Zhi-yong LI, Mao-bing FAN, Sai-long ZHANG, Yi QU, Si-li ZHENG, and Jie SONG performed the experiments.

References

- 1 Jorgensen JR, Fransson A, Fjord-Larsen L, Thompson LH, Houchins JP, Andrade N, *et al*. Cometin is a novel neurotrophic factor that promotes neurite outgrowth and neuroblast migration *in vitro* and supports survival of spiral ganglion neurons *in vivo*. *Exp Neurol* 2012; 233: 172–81.
- 2 Li ZY, Zheng SL, Wang P, Xu TY, Guan YF, Zhang YJ, *et al*. Subfatin is a novel adipokine and unlike Meteorin in adipose and brain expression. *CNS Neurosci Ther* 2014; 20: 344–54.
- 3 Ushach I, Burkhardt AM, Martinez C, Hevezi PA, Gerber PA, Buhren BA, *et al*. METEORIN-LIKE is a cytokine associated with barrier tissues and alternatively activated macrophages. *Clin Immunol* 2015; 156: 119–27.
- 4 Zheng SL, Li ZY, Song J, Liu JM, Miao CY. *Metrn1*: a secreted protein with new emerging functions. *Acta Pharmacol Sin* 2016; 37: 571–9.
- 5 Rao RR, Long JZ, White JP, Svensson KJ, Lou J, Lokurkar I, *et al*. Meteorin-like is a hormone that regulates immune-adipose interactions to increase beige fat thermogenesis. *Cell* 2014; 157: 1279–91.
- 6 Li ZY, Song J, Zheng SL, Fan MB, Guan YF, Qu Y, *et al*. Adipocyte *Metrn1* antagonizes insulin resistance through PPARγ signaling. *Diabetes* 2015; 64: 4011–22.
- 7 Nishino J, Yamashita K, Hashiguchi H, Fujii H, Shimazaki T, Hamada H. Meteorin: a secreted protein that regulates glial cell differentiation and promotes axonal extension. *EMBO J* 2004; 23: 1998–2008.
- 8 Gan L, Meng ZJ, Xiong RB, Guo JQ, Lu XC, Zheng ZW, *et al*. Green tea polyphenol epigallocatechin-3-gallate ameliorates insulin resistance in non-alcoholic fatty liver disease mice. *Acta Pharmacol Sin* 2015; 36: 597–605.
- 9 Murchie R, Guo CH, Persaud A, Muise A, Rotin D. Protein tyrosine phosphatase sigma targets apical junction complex proteins in the intestine and regulates epithelial permeability. *Proc Natl Acad Sci U S A* 2014; 111: 693–8.
- 10 Jin J, Peng C, Wu SZ, Chen HM, Zhang BF. Blocking VEGF/Caveolin-1 signaling contributes to renal protection of fasudil in streptozotocin-induced diabetic rats. *Acta Pharmacol Sin* 2015; 36: 831–40.
- 11 Hu G, Liu J, Zhen YZ, Xu R, Qiao Y, Wei J, *et al*. Rhein lysinate increases the median survival time of SAMP10 mice: protective role in the kidney. *Acta Pharmacol Sin* 2013; 34: 515–21.
- 12 Bade S, Gorris HH, Koelling S, Olivier V, Reuter F, Zabel P, *et al*. Quantitation of major protein constituents of murine intestinal fluid. *Anal Biochem* 2010; 406: 157–65.
- 13 Xu TY, Lan XH, Guan YF, Zhang SL, Wang X, Miao CY. Chronic nicotine treatment enhances vascular smooth muscle relaxation in rats. *Acta Pharmacol Sin* 2015; 36: 429–39.
- 14 Hansson GC. Role of mucus layers in gut infection and inflammation. *Curr Opin Microbiol* 2012; 15: 57–62.
- 15 Johansson ME, Sjovall H, Hansson GC. The gastrointestinal mucus system in health and disease. *Nat Rev Gastroenterol Hepatol* 2013; 10: 352–61.
- 16 Birchenough GM, Johansson ME, Gustafsson JK, Bergstrom JH, Hansson GC. New developments in goblet cell mucus secretion and function. *Mucosal Immunol* 2015; 8: 712–9.

- 17 Kim YS, Ho SB. Intestinal goblet cells and mucins in health and disease: recent insights and progress. *Curr Gastroenterol Rep* 2010; 12: 319–30.
- 18 Johansson ME, Phillipson M, Petersson J, Velcich A, Holm L, Hansson GC. The inner of the two Muc2 mucin-dependent mucus layers in colon is devoid of bacteria. *Proc Natl Acad Sci U S A* 2008; 105: 15064–9.
- 19 Van der Sluis M, De Koning BA, De Bruijn AC, Velcich A, Meijerink JP, Van Goudoever JB, *et al*. Muc2-deficient mice spontaneously develop colitis, indicating that MUC2 is critical for colonic protection. *Gastroenterology* 2006; 131: 117–29.
- 20 Velcich A, Yang W, Heyer J, Fragale A, Nicholas C, Viani S, *et al*. Colorectal cancer in mice genetically deficient in the mucin Muc2. *Science* 2002; 295: 1726–9.
- 21 Bergstrom KS, Kisson-Singh V, Gibson DL, Ma C, Montero M, Sham HP, *et al*. Muc2 protects against lethal infectious colitis by disassociating pathogenic and commensal bacteria from the colonic mucosa. *PLoS Pathog* 2010; 6: e1000902.
- 22 Bevins CL, Salzman NH. Paneth cells, antimicrobial peptides and maintenance of intestinal homeostasis. *Nat Rev Microbiol* 2011; 9: 356–68.
- 23 Gallo RL, Hooper LV. Epithelial antimicrobial defence of the skin and intestine. *Nat Rev Immunol* 2012; 12: 503–16.
- 24 Cash HL, Whitham CV, Behrendt CL, Hooper LV. Symbiotic bacteria direct expression of an intestinal bactericidal lectin. *Science* 2006; 313: 1126–30.
- 25 Burger-van Paassen N, Loonen LM, Witte-Bouma J, Korteland-van Male AM, de Bruijn AC, van der Sluis M, *et al*. Mucin Muc2 deficiency and weaning influences the expression of the innate defense genes Reg3beta, Reg3gamma and angiogenin-4. *PLoS One* 2012; 7: e38798.
- 26 Brandl K, Plitas G, Schnabl B, DeMatteo RP, Pamer EG. MyD88-mediated signals induce the bactericidal lectin RegIII gamma and protect mice against intestinal *Listeria monocytogenes* infection. *J Exp Med* 2007; 204: 1891–900.
- 27 Siqueiros-Cendon T, Arevalo-Gallegos S, Iglesias-Figueroa BF, Garcia-Montoya IA, Salazar-Martinez J, Rascon-Cruz Q. Immunomodulatory effects of lactoferrin. *Acta Pharmacol Sin* 2014; 35: 557–66.
- 28 Reigstad CS, Backhed F. Microbial regulation of SAA3 expression in mouse colon and adipose tissue. *Gut Microbes* 2010; 1: 55–7.
- 29 Vaishnava S, Behrendt CL, Ismail AS, Eckmann L, Hooper LV. Paneth cells directly sense gut commensals and maintain homeostasis at the intestinal host-microbial interface. *Proc Natl Acad Sci U S A* 2008; 105: 20858–63.
- 30 Peterson LW, Artis D. Intestinal epithelial cells: regulators of barrier function and immune homeostasis. *Nat Rev Immunol* 2014; 14: 141–53.
- 31 Wittkopf N, Neurath MF, Becker C. Immune-epithelial crosstalk at the intestinal surface. *J Gastroenterol* 2014; 49: 375–87.